

# Laminar Thermal Mixing in Coating Flows

A. Haas<sup>\*,1</sup>, M. Scholle<sup>1</sup>, N. Aksel<sup>1</sup>, H.M. Thompson<sup>2</sup>, R.W. Hewson<sup>2</sup>, P.H. Gaskell<sup>2</sup>

<sup>1</sup>Department of Applied Mechanics and Fluid Dynamics, University of Bayreuth, D-95440 Bayreuth, Germany

<sup>2</sup>School of Mechanical Engineering, University of Leeds, Leeds LS2 9JT, UK

\*Corresponding author: andre.haas@uni-bayreuth.de

**Abstract:** Heat transfer in a plane shear flow configuration consisting of two infinitely long parallel plates is considered. The upper planar plate drives the flow by a constant velocity, whereas the lower plate is fixed and has a regular sinusoidally varying profile [3]. In laminar flows over undulated substrates eddies can be generated due to the kinematical constraints; details of the genesis and manipulation of which is discussed in [4] and [5].

A closed form analytical solution for the the velocity field, based on lubrication theory as well as a semi-analytic solution, provided by the application of Ritz's direct method, for the temperature field is derived for the creeping flow. Additionally, detailed numerical solutions are obtained via a finite element formulation of the governing equations for mass, momentum and energy conservation, enabling an exploration of the inertial effects.

It is shown that changes in the mean plate separation, that is the geometry, and the level of inertia present affect the local hydrodynamic flow structure in the form of kinematically and inertially induced eddies, respectively. These in turn impact on the local laminar thermal mixing, and consequently enhance the global heat transfer. Resulting Nusselt numbers are reported for a wide range of Peclet and Reynolds numbers with agreement between the two methods of solution, for the case of creeping flow, found to be extremely good.

**Keywords:** Flow structure, Thermal mixing, Heat transfer, Shear flow, Topography

## 1 Introduction

Consider, as illustrated in Fig. 1, the case of steady, two-dimensional Couette flow of an incompressible fluid confined between two infinite, horizontally aligned plates, with the moving upper flat plate, temperature  $T_0$ , separated by a small mean distance from the sta-

tionary lower one which has a regular sinusoidally varying profile and is at temperature  $T_1$ , ( $T_1 > T_0$ ). The fluid properties are taken as those for silicone oil, as used in [6] in the investigation of the corresponding isothermal flow problem. The thermal conductivity,  $\lambda$ , and specific heat,  $c_p$ , are assumed constant, while the density  $\rho$  and viscosity  $\eta$ , have the form

$$\rho(T) = \rho_0 (1 - \beta T) \quad (1)$$

$$\eta(T) = \eta_0 (1 - \eta^* T) \quad (2)$$

with the non-dimensional constants  $\beta$  and  $\eta^*$  denoting the coefficients of thermal expansion and thermoviscosity, respectively.

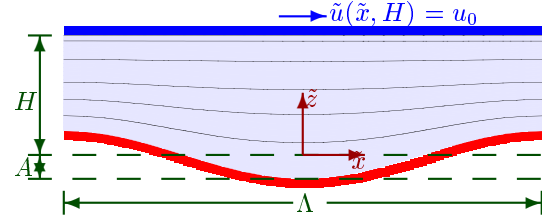


Figure 1: Schematic of the flow geometry

The two coordinates  $\tilde{x}$ ,  $\tilde{z}$  are scaled by  $\Lambda/2\pi$  with  $\Lambda$  being the wavelength. The velocity is scaled by the lid velocity  $u_0$ . Thus, the geometry is characterised by two nondimensional parameters, namely the dimensionless mean plate distance  $h$  and the dimensionless amplitude  $a$ . Additionally, the pressure  $\tilde{p}$  and temperature  $\tilde{T}$  are scaled as follows

$$\tilde{p} = \frac{2\pi\eta_0 u_0}{\Lambda} p; \quad \tilde{T} = T(T_1 - T_0) + T_0 \quad (3)$$

with  $0 \leq T \leq 1$ .

## 2 Governing equations

Within the framework of the Boussinesq approximation the continuity equation in non-dimensional form simplifies to

$$u_x + w_z = 0. \quad (4)$$

By taking  $\Lambda$  to be sufficiently small the system can be defined in such a way that buoyancy effects can be neglected and by a proper choice of the fluid parameters the stability condition for the non occurrence of natural convection can be fulfilled, further details can be found in [3]. In addition thermal expansion plays no part in the flow. Consequently, terms involving  $\beta T$  can be neglected in the Navier–Stokes equations

$$\text{Re} [u u_x + w u_z] = -p_x + 2\partial_x [(1 - \eta^* T) u_x] + \dots \partial_z [(1 - \eta^* T) (u_z + w_x)] \quad (5)$$

$$\text{Re} [u w_x + w w_z] = -p_z + 2\partial_z [(1 - \eta^* T) w_z] + \dots \partial_x [(1 - \eta^* T) (u_z + w_x)] \quad (6)$$

If dissipation is assumed to be negligible, see also [3], the temperature equation reduces to the following form:

$$\text{Pe} [u T_x + w T_z] - [T_{xx} + T_{zz}] = 0 \quad (7)$$

The Reynolds and the Peclét number in the utilised scaling are defined as follows:

$$\text{Re} = \frac{\rho_0 u_0 \Lambda}{2\pi \eta_0}; \quad \text{Pe} = \frac{\Lambda u_0 \rho_0 c_p}{2\pi \lambda} \quad (8)$$

### 3 Boundary conditions

In non-dimensional form the spatial locations of the lower and the upper plates are given by  $z = -a \cos x$  and  $z = h$ , respectively, along which a no-slip condition is applied

$$u(x, -a \cos x) = 0 \quad u(x, h) = 1 \quad (9)$$

$$v(x, -a \cos x) = 0 \quad v(x, h) = 0. \quad (10)$$

For the temperature field the corresponding upper and lower plate conditions are the Dirichlet ones, namely

$$T(x, -a \cos x) = 1; \quad T(x, h) = 0. \quad (11)$$

In addition periodic boundary conditions for all fields to the left and to the right of the flow domain are imposed.

### 4 Semi-analytical solution

For simplification a creeping flow is considered,  $\text{Re} \rightarrow 0$  and thermoviscous coupling terms involving  $\eta^*$  are neglected, leading to an unilaterally coupled problem and the hydrodynamic field can be solved separately from the temperature field.

#### 4.1 Hydrodynamic field

Invoking the lubrication approximation reduces the hydrodynamic problem to the Reynolds' equation, a single ordinary differential equation. Its closed form analytic solution leads to the following explicit expression for the streamfunction  $\psi$  [2],

$$\frac{\psi}{hZ^2} = \frac{h^2 - 4a^2 + 3a^2 Z}{2h^2 + a^2} + \frac{a}{h} (Z - 1) \cos x, \quad (12)$$

by introducing

$$Z = \frac{z + a \cos x}{h + a \cos x} \quad (13)$$

as a new coordinate. The coordinate transformation  $(x, z) \rightarrow (x, Z)$  maps the flow domain of interest sketched in Fig. 1 to a rectangular domain  $[0, 2\pi] \times [0, 1]$ . In the new coordinate system, the lubrication solution for the streamfunction can be written as a non-orthogonal series expansion

$$\psi = (x, Z) = \sum_{n=-1}^{n=1} \psi_n(Z) e^{-inx} \quad (14)$$

with the coefficients

$$\psi_0 = \frac{(h^2 - 4a^2) hZ^2 + 3ha^2 Z^3}{2h^2 + a^2} \quad (15)$$

$$\psi_{\pm 1} = -\frac{a}{2} Z^2 (Z - 1), \quad (16)$$

giving an excellent approximation for small dimensionless amplitudes to  $a \leq 1/2$ .

#### 4.2 Temperature field

The essence of the analysis is the construction of an analogous series representation for temperature as for the streamfunction (14), i.e.

$$T = (x, Z) = \sum_{n=-N}^{n=N} T_n(Z) e^{-inx} \quad (17)$$

with  $N \in \mathbb{N}$ . It can be shown, see [3] that equation (7) results from variation of the functional

$$I = \int_{-\pi}^{\pi} \int_0^1 [ -\text{Pe} T(x, Z) (\mathbf{u} \cdot \nabla) T(-x, Z) + \nabla T(x, Z) \cdot \nabla T(-x, Z)] (h + a \cos x) dZ dx \quad (18)$$

with respect to the temperature, provided that the velocity field is symmetric. For isothermal creeping flow given by equation (12) these conditions are fulfilled. Use of the above variational formulation is advantageous since Ritz's direct method can be applied which represents an efficient means of solution [3].

## 5 Finite element solution

Equations (4)-(7) and the associated boundary conditions (9)-(11) were solved numerically using COMSOL Multiphysics with the comprised *Fluid Dynamics/Incompressible Navier-Stokes* and *Heat Transfer/Convection and Conduction* application modules.

A non-uniform mesh comprised of triangu-

lar elements clustered towards the lower plate was used to discretise the flow domain, employing second order interpolation functions for velocities and temperature and first order interpolation for pressure. The resulting system of equations was solved iteratively using a form of the damped Newton method as described in [1]. The problem was programmed in the MATLAB environment to allow for the flexible control of geometric and fluid parameters. A variety of mesh densities was examined to establish the number and distribution of elements required to guarantee mesh independent solutions for the parameter range investigated. For a typical flow geometry with  $a = 1/2$  and  $h = 3/4$  the number of elements required to ensure mesh independence was found to be 275710.

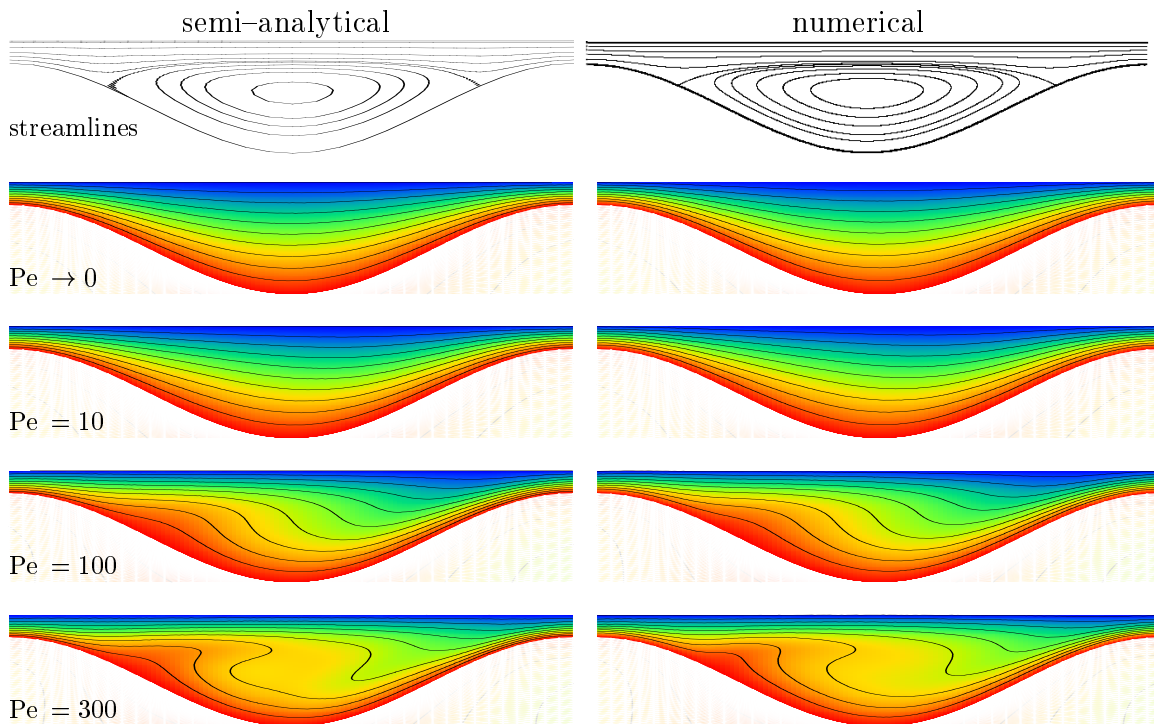


Figure 2: Flow structure (streamlines) and corresponding temperature field (isotherms) transition with increasing  $Pe$ , obtained semi-analytically (left) and numerically (right), for the case  $a = 1/2$ ,  $h = 3/4$  [3].

## 6 Results and discussion

Results for creeping flow and flow with inertia are presented independently of each other.

### 6.1 Creeping flow

#### 6.1.1 Temperature field

Fig. 2, for the case  $a = 1/2$  and a mean plate separation of  $h = 3/4$ . These were obtained:

(i) using the semi-analytical approach, with  $N = 4$  modes for the series (17); (ii) numerically as described above. Agreement between the two sets of results is seen to be remarkably close, with the streamline plots showing that the geometry as specified results in the presence of a large symmetric eddy while the nature of the corresponding temperature field is Peclet number dependent. When  $Pe = 0$  the problem is one of pure heat conduction and the temperature field is symmetric as shown. Symmetry is, however, soon lost due to the presence of convection as demonstrated for the case  $Pe = 10$ . As  $Pe$  is increased further a point is soon reached, when for sufficiently large values, see for example the case  $Pe = 100$ , the asymmetry present becomes pronounced as warmer fluid is transported upwards on the left side of the domain with a corresponding downward movement of colder fluid on the right. For Peclet numbers of approximately 300 and greater, the isotherms mimic the corresponding streamline pattern with laminar thermal mixing occurring.

### 6.1.2 Global heat transport

A measure for the global heat transport is provided by the Nusselt number  $Nu$  which is found from the temperature field as

$$Nu = -\frac{h}{2\pi} \int_{-\pi}^{\pi} T_z|_{z=h} dx \quad (19)$$

It represents the non-dimensional global heat flux, scaled with the corresponding heat flux  $\lambda(T_1 - T_0)/h$  for Couette flow between parallel flat plates fixed at the same reference temperatures and in which case  $Nu = 1$ .

The Nusselt number was calculated both semi-analytically and numerically for the case of a bottom plate with amplitude  $a = 1/2$  and for different mean plate separations, the results of which are plotted against Peclet number in Fig. 3. Values of  $h$  were chosen in such a way that four qualitatively different cases could be investigated: one without an eddy present ( $h = 7/4$ ), a second exhibiting a small eddy ( $h = 1$ ), the third with a large eddy present ( $h = 3/4$ ), and a fourth case in which the flow has all but degenerated to that of a driven-cavity like flow consisting almost entirely of a large single eddy ( $h = 3/5$ ).

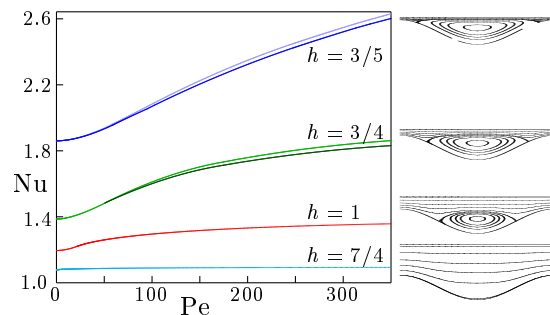


Figure 3: Global heat transport depicted as plots of Nusselt number vs. Peclet number for the case of a lower plate with amplitude  $a = 1/2$  and four different mean plate separations. The upper curves represent the results obtained semi-analytically [3].

In all cases the analytical and numerical results are in very good agreement with each other. Compared to the case of parallel plates ( $Nu = 1$ ), it can be seen that there is already an improvement in the global heat transport for  $Pe \rightarrow 0$ ; that is, even in the case of pure heat conduction it is observed that  $Nu > 1$  as a consequence of the geometry.

For  $Pe > 0$  an additional increase in  $Nu$ , due to convection, is apparent. This effect, however, depends significantly on the eddy size: for the case  $h = 7/4$ , one without an eddy, only a tiny improvement in the heat flux is observed, whereas the curve corresponding to the flow containing a small eddy ( $h = 1$ ) reveals a distinct gradual increase of the Nusselt number with increasing  $Pe$ . This effect becomes even more pronounced the larger the eddy ( $h = 3/4$ ) and especially so in the case of a driven-cavity like flow ( $h = 3/5$ ).

### 6.1.3 Thermal feedback on the flow

Thermal feedback due to thermoviscosity  $\eta = \eta(T)$  is investigated numerically, with buoyancy and thermal expansion effects due to  $\rho = \rho(T)$  neglected, as discussed in Section 2. In Fig. 4 results are shown for the case  $a = 1/2$ ,  $h = 3/4$ , a Peclet number  $Pe = 100$  and a thermoviscous coupling with  $\eta^* = 1/3$  corresponding to a temperature-dependent viscosity given by

$$\eta(T) = \eta_0 \left[ 1 - \frac{T}{3} \right] \quad (20)$$

Note that this choice of temperature dependence leads to a fluid viscosity that is 50%

larger at the colder plate than at the warmer one. Hence, a strong thermoviscous coupling is implicit in the calculations. For comparison purposes streamlines and isotherms are shown for the case of constant viscosity. Shown also is the constant viscosity case when the temperatures of the plates are reversed that is, the top plate is hotter than the bottom one. The surprising result which emerges from this figure is that, even in the case of strong thermoviscous

coupling, the feedback effect of the temperature on the flow is negligibly small. Moreover, by comparing the resulting temperature fields there is no discernible difference, even in the case when the temperatures of the upper and lower plates are reversed. Accordingly, this result supports the a priori assumption made when formulating the semi-analytical method of solution that the flow and temperature fields can be decoupled.

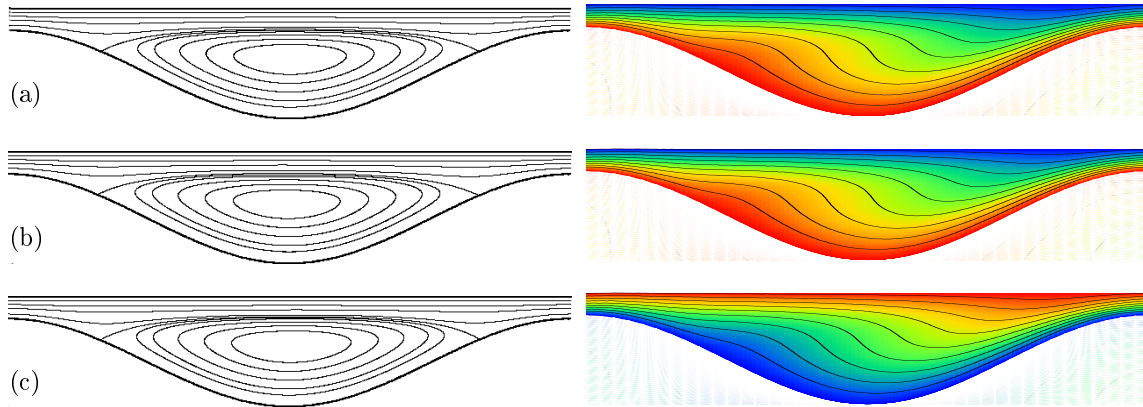


Figure 4: Numerically calculated streamlines (left) and corresponding isotherms (right) for a flow geometry with  $a = 1/2$  and  $h = 3/4$ , and  $Pe = 100$ : (a) constant viscosity; (b) viscosity according to equation (20); (c) as (a) but with the upper and lower plate temperatures reversed [3].

## 6.2 Flow with finite Reynolds number

### 6.2.1 Effect of increasing inertia

Numerical solutions were obtained, see Fig. 6, for Stokes flow and at Reynolds number  $Re = 100$  for the case  $a = 1/2$  and the same four mean plate separations as considered in Fig. 3, and with  $Pe = 100$ . The streamline plots to the left, for Stokes flow, show the influence of the mean plate separation, that is the geometry, on the eddy structure present; those on the right, for the case  $Re = 100$ , reveal that the presence of inertia can lead to both eddy generation and to increased asymmetry of an existing eddy structure. The shift in the vortex core, in the case of the latter, has consequences for the corresponding temperature field: in that the area where the heat transport due to convection is significant is also shifted to the right.

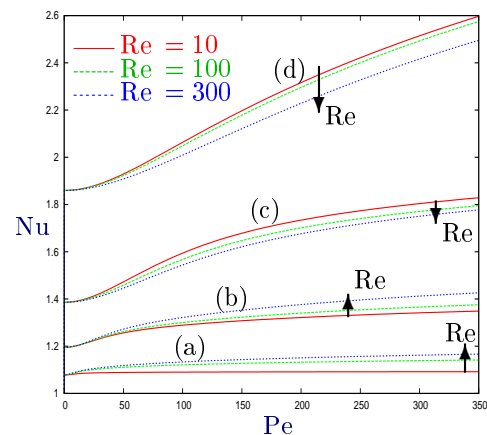


Figure 5: Global heat transport depicted as plots of Nusselt number vs. Peclet number, at three different Reynolds numbers, for a lower plate with amplitude  $a = 1/2$  and the four mean plate separations (a)–(d) used in Figure 3, see [3].

## 6.2.2 Global heat transport

Using equation 19 the Nusselt number was calculated for the case of a lower plate with amplitude  $a = 1/2$ , for the same four mean plate separations. This was done at three different Reynolds numbers  $Re = 10, 100, 300$  for Peclet numbers between 0 and 350. The resulting curves of  $Nu$  versus  $Pe$  are shown in Fig. 5. Compare these with those in Fig. 3 for the corresponding creeping flow problem. The effect of inertia is qualitatively different for the four geometries considered: in the two cases (d) and (c) commensurate with a smaller mean plate separation,  $h = 3/5$  and  $h = 3/4$ , respectively, the global heat transport is reduced with increasing inertia, whereas in the

two cases (b) and (a) with a larger mean plate separation,  $h = 1$  and  $h = 7/4$  respectively, the opposite occurs and it is enhanced. The explanation for this qualitative difference is found by examining the underlying flow structures. In the case  $h = 3/4$ , for instance, the corresponding velocity field shown in Fig. 6 reveals a shift to the right of the vortex core. Therefore, the area over which convective heat transport is relevant is reduced. The same qualitative effect is found for  $h = 3/5$ , since in this case too there is a large eddy in the flow. In contrast, for  $h = 1$  there is only a small eddy present, while for  $h = 7/4$  there is no eddy present at assisting the transport of heat which shows as a corresponding increase in the Nusselt number.

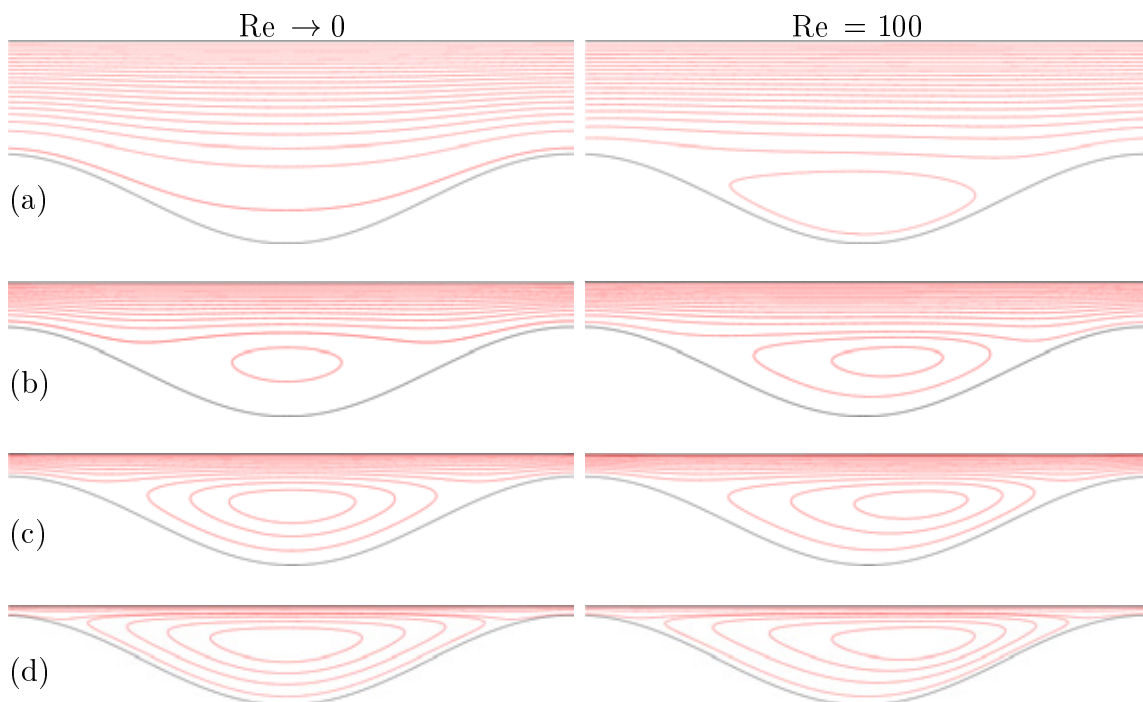


Figure 6: Numerically calculated streamlines (left) and corresponding isotherms (right) for a flow geometry with  $a = 1/2$  and  $h = 3/4$ , and  $Pe = 100$ : (a) constant viscosity; (b) viscosity according to equation (20); (c) as (a) but with the upper and lower plate temperatures reversed [3].

## 7 Conclusion

The subtle interplay that exists between the global transfer of heat and the underlying flow structure and hence local laminar thermal mixing in the case of shear flow between two rigid surfaces at different fixed temperatures – the hot, upper one, planar; the lower, cooler one, varying sinusoidally – a small mean dis-

tance apart, has been explored both analytically and numerically. For creeping flow conditions and varying Peclet number, the thermal field is found to be asymmetric for all values of the Peclet number other than the limiting conditions of zero and infinity, at which extremes the corresponding thermal field is symmetric.

Global heat transport, in the form of plots of Nusselt number against Peclet number, is

investigated with agreement between predictions from analysis and ones obtained numerically seen to be extremely good, particularly for higher values of mean plate separation. It is found that compared to the case when both top and bottom plates are flat there is an improvement to be seen in global heat transport as a consequence of the geometry, even for the case of pure heat conduction ( $Pe \rightarrow 0$ ), but which depends significantly on the size of the underlying eddy structure present as the Peclet number is increased and convection plays a more significant role.

In the case of non-creeping flow, the effect of increasing inertia on both the temperature field and global heat transport is revealed, the obvious one being to skew the underlying eddy structure – for moderate Reynolds numbers,  $Re = 100$ , this takes the form of a shift to the right of the vortex core. The consequence for the corresponding temperature fields is that the region where heat transfer due to convection is significant is also skewed in the same direction. The results obtained for global heat transfer expose the interrelationship between eddies induced kinematically and due to inertia, in that inertia can result in the creation of an eddy or enlarge an existing eddy, for a given lower plate profile and mean plate separation, that is fixed flow geometry. Indeed the present work suggests that for a given sinusoidal variation of the lower plate it should be possible, from a practical standpoint, to find a critical mean plate separation for which Reynolds number effects on the global heat transfer are

minimised.

## References

- [1] P. Deuffhard, *A modified newton method for the solution of ill-conditioned systems of nonlinear equations with application to multiple shooting*, *Numerische Mathematik* **22** (1974), no. 4, 289–315.
- [2] M. Scholle, *Creeping couette flow over an undulated plate*, *Arch. Appl. Mech.* **73** (2004), 823–840.
- [3] M. Scholle, A. Haas, N. Aksel, H.M. Thompson, R.W. Hewson, and P.H. Gaskell, *The effect of locally induced flow structure on global heat transfer for plane laminar shear flow*, *International Journal of Heat and Fluid Flow* **30** (2009), no. 2, 175–185.
- [4] M. Scholle, A. Haas, N. Aksel, M. C. T. Wilson, H. M. Thompson, and P. H. Gaskell, *Competing geometric and inertial effects on local flow structure in thick gravity-driven fluid films*, *Physics of Fluids* **20** (2008), no. 12, 123101–10.
- [5] ———, *Eddy genesis and manipulation in plane laminar shear flow*, *Physics of Fluids* **21** (2009), no. 7, 073602–12.
- [6] A. Wierschem, M. Scholle, and N. Aksel, *Vortices in film flow over strongly undulated bottom profiles at low reynolds numbers*, *Phys. Fluids* **15** (2003), 426–435.